Comparison of General Multi-Carrier Schemes in Two Way Relaying Channels

Matthias Woltering, Ming Zhang, Dirk Wübben, and Armin Dekorsy
University of Bremen, Bremen, Germany
Email: {woltering, zhang, wuebben, dekorsy}@ant.uni-bremen.de

***Abstract*—In this paper multi-carrier transmission schemes applying general waveforms are discussed within two-phase two way relay channels. Here, two users communicate simultaneously on the same resources to an assisting relay. The relay has to cope with the superposition of both users, interferences of the channel and additional practical impairments like frequency and timing offsets. To be more robust against these impairments, Filter Bank Multi-Carrier (FBMC) systems with general waveforms are used. They offer better time-frequency properties by the cost of additional interference introduced by the waveforms than CP-OFDM applying rectangular waveform. The main contribution of this work is the performance analysis w.r.t. the sensitivity against phase differences of the user channels in FBMC with QAM and Offset-QAM (OQAM) modulation. BER performance analysis show that under realistic channel conditions QAM/FBMC outperforms OFDM as well as OQAM/FBMC with one antenna at the relay. If the relay use an additional antenna at the relay, the multi-carrier applying OQAM outperforms QAM modulation. Hence, the choice of OQAM or QAM depends on the number of antennas available at the relay.**

I. Introduction

FBMC transmission schemes are promising candidates for future mobile communication systems [1], [2]. In contrast to OFDM with Cyclic Prefix (CP) applied in LTE, DVB-T, WLAN (802.11 a/g) and other standards, where rectangular waveforms are used, general waveforms used in FBMC, offer better time-frequency properties and, thus, higher robustness to channel time variations.

In this work, we consider two-phase Two Way Relay Channel (TWRC) communication, where two users simultaneously exchange data over an assisting relay in the Multiple Access Channel (MAC) phase. The spectral efficiency is significantly improved by assisted relays [3], decreasing the path loss and offering spatial diversity. The relay estimates a joint message based on the received signal, which will be transmitted in the Broadcast (BC) phase. Due to the transmission at the same time on the same frequency resource, a superposition of both user signals affected by individual channels and offsets is received at the relay. The performance of CP-OFDM in this setting was analyzed in [4], [5]. Here, it was shown that CP-OFDM suffers from time-variant channels or from practical constraints like Carrier Frequency Offset (CFO), which cannot be completely removed within TWRCs. To combat the weakness of CP-OFDM, QAM/FBMC within TWRC has been analyzed in [6]–[8]. FBMCs is in general more robust considering practical influences as conventional CP-OFDM [2], [9]. Applying Offset-QAM (OQAM) modulation to FBMC leads to so-called OQAM/FBMC. The main advantage of this combination is the reduction of internal interference introduced by the general waveform since the interference is shifted into imaginary part of the signal.

In this paper non-orthogonal QAM/FBMC, the interference reduced version OQAM/FBMC and OFDM will be compared within TWRCs w.r.t. phase differences between users. By numerical evaluations, the BER performance of the different schemes is analyzed applying different detection schemes at the relay.

The paper is organized as follows: Section II gives a brief overview of the transmit signals per user over the considered multi-carrier waveform schemes. In Section III the overall system model of a two-phase TWRC is introduced in matrix description. This model describes the impact of doubly dispersive channels the overall used Transmitter/Receiver (Tx/Rx) filters as well as the considered detection methods, and it gives first indications on the effects of phase differences within TWRCs. To reduce the introduced interference by non-orthogonal waveforms as well as interference introduced by the channel, Section III-B deals with equalization techniques designed for TWRCs. The Bit Error Rate (BER) performance of the different multi-carrier schemes and the different detection schemes will be compared intensively by link level simulations in Section IV. Section V concludes the paper and gives a short outlook on future work.

II. Signal generation

As illustrated in Fig. 1 two users A and B encode their information vectors $\mathbf{u}_i$, $i \in \{\mathrm{A}, \mathrm{B}\}$ by a linear encoder to the code words $\mathbf{c}_i$. The modulator maps the code words to a symbol matrix $\mathbf{D}_i$ with size $N_k \times N_\ell$, where N_k is the number of sub-carriers and N_ℓ is the number of occupied time instances. Each complex symbol $d_i^{(k,\ell)}$ within the matrix $\mathbf{D}_i$ is an M-QAM modulated symbol shifted to the time-frequency point (k, ℓ) by a general transmit waveform given by

$$g_{\mathrm{Tx}}^{(k,\ell)}(t) = g_{\mathrm{Tx}}(t - \ell T_0)\, \mathrm{e}^{j2\pi k F_0 t}, \qquad (1)$$

where ℓT_0 is the time symbol spacing and kF_0 is the sub-carrier spacing.

In this paper, we focus on the following Tx/Rx filters.

1) Rectangular filter used in OFDM or CP-OFDM, fulfill-

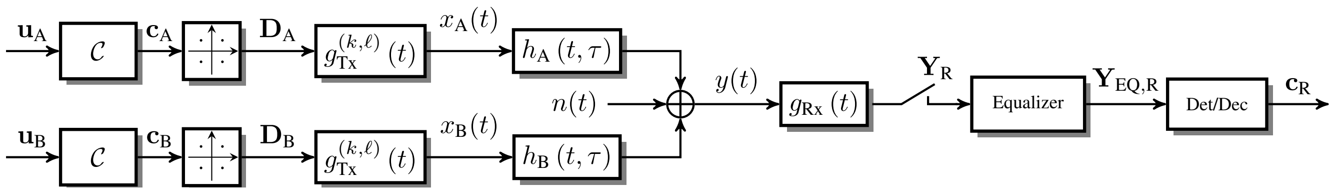

Fig. 1. Block diagram of the MAC phase used a relay with one antenna at the relay

ing 1.Nyquist criteria.

$$g_\mathrm{Tx}(t) = \begin{cases} 1/\sqrt{T_0} & |t| \geq T_0/2 \\ 0 & \text{otherwise} \end{cases} \tag{2}$$

2) Squared Root Raised Cosine (SRRC) filter with roll-off factor r:

$$g_\mathrm{Tx}(t) = \frac{\sin\left((1-r)\frac{\pi t}{T_0}\right) + 4r\frac{t}{T_0}\cos\left((1+r)\frac{\pi t}{T_0}\right)}{\sqrt{T_0}\frac{\pi t}{T_0}\left(1-\left(\frac{4rt}{T_0}^2\right)\right)} \tag{3}$$

3) The non-orthogonal Gaussian filter with localization parameter α:

$$g_\mathrm{Tx}(t) = (2\alpha)^{1/4}\mathrm{e}^{-\pi\alpha t^2} \quad . \tag{4}$$

A general non-orthogonal waveform $g_\mathrm{Tx}(t)$ like (4) introduces interference into the multi-carrier system, but can offer flexible and adaptable localization properties in time and frequency direction. The Balian-Low theorem [10] states that an orthogonal basis is not possible with a well-localized filter, if the time frequency density is $F_0T_0 = 1$. However, especially under practical constraints e.g. Timing Offsets (TOs), CFOs, Doppler spread or time spreads, a well-localized filter only introduces interference to the adjacent time-frequency points.

A. QAM Filter Bank Multi-Carrier Transmission

The transmit signal of user i is given by the summation of the complex data symbols shifted to the corresponding time-frequency point by

$$x_i(t) = \sum_{k=0}^{N_k-1}\sum_{\ell=0}^{N_\ell-1} d_i^{(k,\ell)} g_\mathrm{Tx}^{(k,\ell)}(t) \quad . \tag{5}$$

With a rectangular waveform defined in (2) and applying additionally a CP this corresponds to the well-known orthogonal CP-OFDM transmission. If the delay spread does not exceed the CP no Inter-Symbol Interference (ISI) is introduced. Thus, simple one-tap equalization for block-fading channels is sufficient. However, the performance of OFDM with CFO or doubly-dispersive channels the performance decreases significantly [5]. And other waveforms offer better performance like in [6], [8], [11].

B. Offset-QAM Filter Bank Multi-Carrier Transmission

When using OQAM modulation, a shift of 50% of the symbol duration T_0 between real and imaginary components is introduced leading to

$$x_i(t) = \sum_{k=0}^{N_k-1}\sum_{\ell=0}^{N_\ell-1} \exp\left(j(\ell+k)\frac{\pi}{2}\right) \times \left[d_{\mathrm{Re},i}^{(k,\ell)} g_\mathrm{Tx}^{(k,\ell)}(t) + d_{\mathrm{Im},i}^{(k,\ell)} g_\mathrm{Tx}^{(k,\ell)}\left(t - \frac{T_0}{2}\right)\right] . \tag{6}$$

Where, $d_{\mathrm{Re},i}^{(k,\ell)}$ determines the real part and $d_{\mathrm{Im},i}^{(k,\ell)}$ the imaginary part of the user symbol $d_i^{(k,\ell)}$. The factor $\exp\left(j(\ell+k)\frac{\pi}{2}\right)$ leads to alternating purely real or purely imaginary symbols in the time-frequency grid. This shifts the interference of the direct neighbors in the time-frequency grid introduced by the general waveform to the imaginary part [1]. At the receiver, the conjugated factor $\exp\left(-j(\ell+k)\frac{\pi}{2}\right)$ is applied and by taking the real part operator the interference in case of a Point-to-Point (P2P) transmission is suppressed totally [2]. Thus, if waveforms only introduce interference to the adjacent neighbors in the time-frequency grid the system can suppress the internal interference totally and an orthogonal system is achieved.

III. Relay Processing

Especially, in TWRCs a robust design of the transmission scheme against practical influences is important since the channel influence can not be reduced individually, but rather jointly [5]. Subsequently, we focus on robust design in multi-carrier schemes within TWRCs.

A. System Model at the Relay

In TWRCs two users A and B exchange data over a relay R with each other. The users are equipped with one antenna, whereas the relay is equipped with either one or two antennas. All nodes are restricted to the half duplex constraint. Here, we assume a two phase transmission, where in the MAC phase both users transmit their data simultaneously to the relay forming a Physical-Layer Network Coding (PLNC) message based on the superposition of channel disturbed signals of both users. Hence, both user signals $x_i(t)$, $i \in \{\mathrm{A},\mathrm{B}\}$ will be affected by doubly-dispersive channels, described by the delay-Doppler function $H_i(t,\tau)$ given by

$$H_i(\tau,t) = \sum_{\iota=0}^{N_\mathrm{h}-1} h_\iota^{(i)}\delta\left(\tau - \tau_\iota^{(i)} - \Delta\tau^{(i)}\right) \times \delta\left(\nu - \nu_\iota^{(i)} - \Delta\nu^{(i)}\right) , \tag{7}$$

and superimposed at the relay. The specific frequency and time selective channel for user i is assumed to have N_h different

TABLE I
PARAMETER SETTING FOR EFFECTIVE CHANNEL IN (10)

scheme	sample time T_0	phase ψ
QAM/FBMC	$T = T_0$	$\psi = 0$
OQAM/FBMC	$T = \frac{T_0}{2}$	$\psi = \frac{\pi}{2}(k - k' + \ell - \ell')$

channel tabs with a complex channel gain $h_\iota^{(i)}$, delay spread $\tau_\iota^{(i)}$, Doppler spread $\nu_\iota^{(i)}$ and additional practical imperfections like a user specific CFO $\Delta\nu^{(i)}$ and TO $\Delta\tau^{(i)}$. After filtering at the receiver with

$$g_{\text{Rx}}^{(k',\ell')}(t) = g_{\text{Rx}}(t - \ell' T_0)\, \mathrm{e}^{j2\pi k' F_0 t}, \tag{8}$$

and sampling with T at the receive time-frequency point (k', ℓ'), the received signal vector $\mathbf{y}_\text{R}$ of a frame is achieved at the relay in matrix description as

$$\mathbf{y}_\text{R} = \mathbf{V}_\text{A}\mathbf{d}_\text{A} + \mathbf{V}_\text{B}\mathbf{d}_\text{B} + \mathbf{n}_\text{R}, \tag{9}$$

where $\mathbf{d}_i \in \mathbb{C}^{N_k N_\ell \times 1}$ is a stacked data vector of user $i \in \{\text{A}, \text{B}\}$ and can be generated by $\mathbf{d}_i = \text{vec}\{\mathbf{D}\}$. The effective channel $\mathbf{V}_i \in \mathbb{C}^{N_k N_\ell \times N_k N_\ell}$ combines the effect of the Tx/Rx filter from (1) and (8) as well as the impact of the doubly-dispersive channel introduced in (7). The (κ, ρ) element $\upsilon^{(\rho,\kappa)}$ (omitting the user index i for simplicity) of the channel matrix $\mathbf{V}_i$ is given in (10) for QAM/FBMC and the OQAM/FBMC transmission with the additional parameters given in Table I. Here, we use the short hand notations $(\rho = k + \ell N_k, \kappa = k' + \ell' N_k)$ to keep a simple nomenclature. Main difference between both schemes is the sample time T and the shifted symbols in the imaginary plain. Particularly, the impact of Tx/Rx filters under frequency and time shifts is described by the ambiguity function $A_g^*(\tau, \nu)$ in (10) and is further discussed in [6]–[8].

B. Equalization

The goal of the linear equalizer is to reduce the interference coming from the other time-frequency points introduced by specific waveforms and the channel. Thus, the linear equalizer minimizes the error $e^{(\kappa)}$ of the (k', ℓ') receive symbol $e^{(\kappa)} = \mathbf{z}^H \mathbf{y}_\text{R} - d^{(\kappa)}$ in Minimum Mean Square Error (MMSE) sense for QAM/FBMC like [6]:

$$\mathbf{z}_{\text{MMSE}}^{(\kappa)} = \arg\min_{\mathbf{z}} \mathrm{E}\left\{ |\mathbf{z}^H \mathbf{y}_\text{R} - d^{(\kappa)}|^2 \right\} \quad . \tag{11}$$

In TWRC, one observation per superposition of user A and B is achieved at the relay, thus the error is calculated based on the superposition

$$d^{(\kappa)} = d_\text{A}^{(\kappa)} + d_\text{B}^{(\kappa)} \quad . \tag{12}$$

As indicated in [7], the output at the equalizer suffers a residual phase term between the transmitted symbols. However, in Subsection III-D detection methods are described based on this superposition.

In case of OQAM/FBMC the useful power should be transmitted in the real domain. In [12], a sub-carrier wise equalization technique for OQAM/FBMC is proposed, however, it still suffering on the residual phase term. Especially, if two users signals are affected by different phases, the derotation can not be resolved individually.

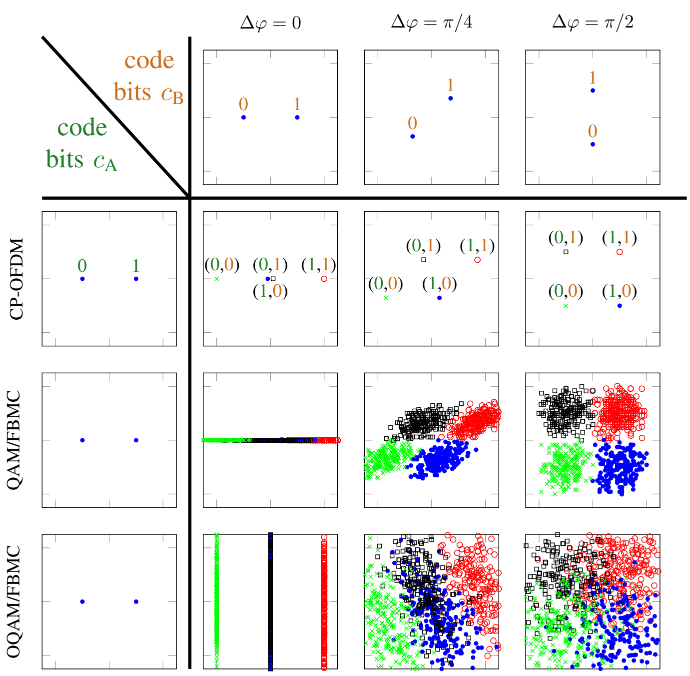

Fig. 2. IQ diagrams of the superposition $\mathbf{y}$ at the relay w.r.t. different phase distortions without additional noise

C. Received Signal

Subsequently, we illustrate the impact of the chosen multi-carrier schemes on the received signal vector $\mathbf{y}_\text{R}$ before equalization at the relay in case of varying phase condition between $H_\text{A}(t, \tau)$ and $H_\text{B}(t, \tau)$ for 1) CP-OFDM, 2) QAM/FBMC with an isotropic Gaussian waveform $\alpha = 1$ and 3) OQAM/FBMC with SRRC waveform with roll-off factor $r = 1$. The channel impulse responses in time domain of user A and B are not changing over time and fixed to

$$\begin{aligned} h_\text{A}(\tau) &= \delta(\tau)\, \mathrm{e}^{j\alpha} \\ h_\text{B}(\tau) &= \delta(\tau)\, \mathrm{e}^{j\beta}. \end{aligned} \tag{13}$$

The channels of the users have only a phase difference $\Delta\varphi = \alpha - \beta$. Without loss of generality, we assume that the phase of user A is fixed $\alpha = 0$ and only phase β is changing. Assuming BPSK modulation for simplicity, Fig. 2 indicates the impact of the phase rotation on the transmitted signals of user B, where the provided labels indicate the bit to symbol mapping.

For the different multi-carrier schemes the impact of the phase rotations on the superimposed signal is visualized by IQ diagrams in the right lower part. In case of CP-OFDM discrete points are achieved and labeled by the corresponding pair of code bits (c_A, c_B). In contrast, QAM/FBMC introduces interference leading to smearing signal points. The actual phase rotation does not affect the amount of interference.

Finally, in case of OQAM/FBMC without phase difference $(\Delta\varphi = 0)$ three straight lines are achieved in the signal space. By considering only the real part of the signals we would achieve the same discrete points as in CP-OFDM.

$$\upsilon^{(\kappa,\rho)} = \sum_{\iota=0}^{N_{\mathrm{h}}-1} h_\iota \cdot \mathrm{e}^{-j2\pi\left(kF_0(\tau_\iota+\Delta\tau)+\left((k'-k)F_0-(\nu_\iota+\Delta\nu)\right)\left(\frac{1}{2}\left((\ell+\ell')T+(\tau_\iota+\Delta\tau)\right)\right)\right)}$$
$$\times A_g^*\left((\ell-\ell')T+(\tau_\iota+\Delta\tau),(k-k')F_0+(\nu_\iota+\Delta\nu)\right)\cdot \mathrm{e}^{\psi}. \quad (10)$$

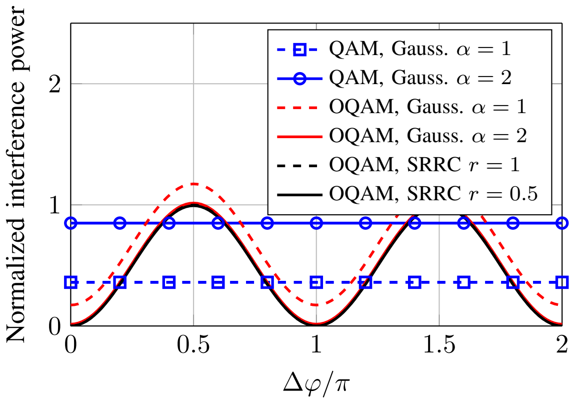

Fig. 3. Interference level of the different multi-carrier schemes with different filter parameters over the phases given by (14) and (15)

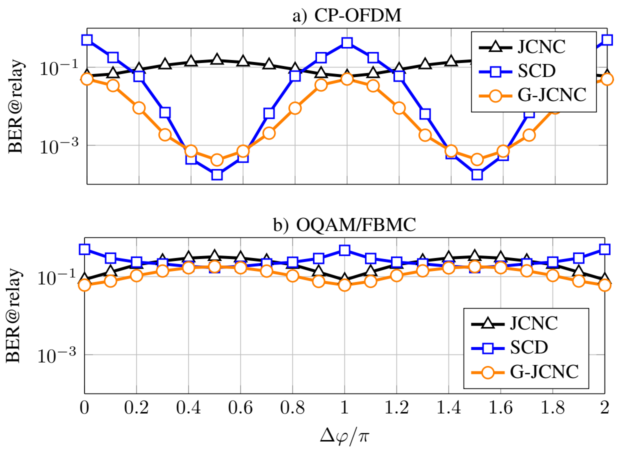

Fig. 4. BER performance of the detection schemes at the relay with different phases $\Delta\varphi$ with a) OFDM [14] b) OQAM/FBMC with an SNR of 7dB

However, with phase differences a huge amount of interference calculated either with (14) for QAM/FBMC or with (15) for OQAM/FBMC is caused by this superposition as also shown in Fig. 3.

$$P^{(\kappa)}_{\mathrm{QAM,I}} = \sigma_{\mathrm{d}}^2 \sum_{\rho\neq\kappa} \left|\upsilon_{\mathrm{A}}^{(\kappa,\rho)}\right|^2 + \sigma_{\mathrm{d}}^2 \sum_{\rho\neq\kappa} \left|\upsilon_{\mathrm{B}}^{(\kappa,\rho)}\right|^2 \quad (14)$$

$$P^{(\kappa)}_{\mathrm{OQAM,I}} = \sigma_{\mathrm{d}}^2 \sum_{\rho\neq\kappa} \left|\Re\left\{\upsilon_{\mathrm{A}}^{(\kappa,\rho)}\right\}\right|^2 + \sigma_{\mathrm{d}}^2 \sum_{\rho\neq\kappa} \left|\Re\left(\upsilon_{\mathrm{B}}^{(\kappa,\rho)}\right)\right|^2 \quad (15)$$

Here the interference level is shown with the channels used in (13). It can be observed that QAM/FBMC with Gaussian waveform suffers a constant interference level independent of the phase difference $\Delta\varphi$ and the minimum interference level is achieved with $\alpha = 1$.

As stated in Section II, OQAM/FBMC is perfectly orthogonal, if localized filters like the SRRC filter with $r = 0.5$ or $r = 1$ is used. For TWRC, this is only true, if the phase difference of the channels is $\Delta\varphi = 0$ or $\Delta\varphi = \pi$. Otherwise, the interference increases dramatically in OQAM/FBMC. Thus, considering only the real part is no longer adequate as this suppresses too much useful information. Within OQAM/FBMC the SRRC Tx/Rx filter with roll-off factor $r = 1$ achieves lower interference power than the Gaussian waveform with $\alpha = 2$. Hence, OQAM/FBMC within the performance analysis part OQAM/FBMC will apply SRRC Tx/Rx filters, in contrast, QAM/FBMC uses the Gaussian waveform.

D. Detection Schemes

Based on the equalized signal $\mathbf{Y}_{\mathrm{EQ,R}}$, the relay estimates a joint message $\mathbf{c}_{\mathrm{R}}$, which should be transmitted in the BC phase [13], [14]. In this paper, we consider three different detection schemes. In Separate Channel Decoding (SCD), the relay detects the code bits c_{A} and c_{B} of each user individually and generates a network coded bit $c_{\mathrm{R}} = c_{\mathrm{A}} \oplus c_{\mathrm{B}}$ by applying the XOR operator. The detection schemes Joint Channel Decoding and Physical-Layer Network Coding (JCNC) and Generalized JCNC (G-JCNC) directly estimate the network coded message c_{R}. JCNC works in the same Galois field as the encoder, whereas G-JCNC exploits higher Galois fields. The performance of all schemes are sensitive against phase rotations [14]. In Fig. 4(a) the BER performance of CP-OFDM w.r.t. phase difference is shown, applying BPSK and the channels in (13) SCD suffers from the impossible separation of the code bits c_{A} and c_{B} in case of $\Delta\varphi = 0$, where JCNC and G-JCNC achieves almost the same performance. The performance of SCD and G-JCNC improves with higher $\Delta\varphi$. With $\Delta\varphi = 0.5$ the best performance is achieved, here the maximum euclidean distance of the possible discrete code bit pairs $(c_{\mathrm{A}}, c_{\mathrm{B}})$ of the discrete points is achieved in the IQ diagram (in Fig. 2), whereas, the BER performance of JCNC is degrading. In contrast, Fig. 4(b) shows the performance of OQAM/FBMC with SRRC. For no phase rotation, all detection schemes in OQAM/FBMC achieves similar BER performances for all detection schemes compared to Fig. 4(a). As expected, the performance of all schemes suffer from the internal interference with phase rotation. Subsequently, we focus more general channels resulting in arbitrary amplitudes and phase values of each user.

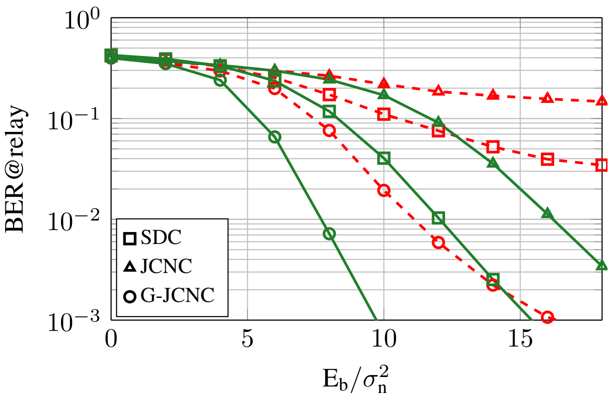

Fig. 5. BER performance of PLNC detection schemes in OQAM/FBMC (solid) and QAM/FBMC (dashed). Channel with $\tau_{\max} = 0.1F_0$ and $\nu_{\max} = 0$, CFO $\Delta\nu = 0$.

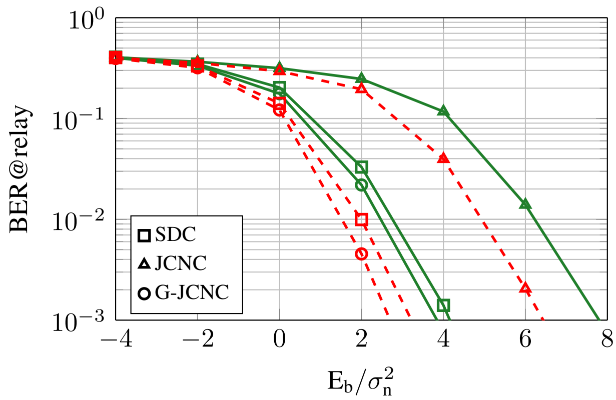

Fig. 6. Comparison of detection schemes in two-way relay with 2 antennas in QAM/FBMC (solid) and OQAM/FBMC (dashed) Channel with $\tau_{\max} = 0.2T_0$ and $\nu_{\max} = 0$, CFO $\Delta\nu = 0$

IV. Performance Evaluation

For the performance evaluation the multi-carrier schemes with QPSK modulation are considered, where a generic channel with N_h complex Rayleigh distributed channel coefficient h_ι are assumed. The time delay τ_ι and the Doppler shift of channel tap h_ι are equally distributed within a range of $[0, \tau_{\max}]$ and $[-\nu_{\max}, \nu_{\max}]$, respectively. In total, 16 subcarriers and 10 time symbols are used to generate a frame containing 160 data symbols.

Fig. 5 shows the BER performance at the relay of the different PLNC detection schemes introduced in Subsection III-D within the both considered multi-carrier schemes QAM/FBMC and OQAM/FBMC with a delay spread of $\tau_{\max} = 0.1T_0$ and no additional impact. All detection schemes with OQAM/FBMC suffer from their additionally introduced interference, thus QAM/FBMC always outperforms OQAM/FBMC. Especially, the G-JCNC shows the best BER performance at the relay due to utilizing the superposition in higher Galois fields.

In contrast to that, in Fig. 6, the BER performance is turning in favor of OQAM/FBMC allowing an additional antenna at the relay. With the additional receive signal of antenna two, the equalizer is able to resolve the phase difference between the users and therefore considering the real part of the equalized signal is sufficient. G-JCNC still outperform the other schemes, however the gain to SCD is significant lower.

Fig. 7(a) shows the BER performance at the relay for QAM/FBMC and OQAM/FBMC with one antenna at the relay using only G-JCNC as detection scheme compared to OFDM. For these simulations, the maximum time delay and maximum Doppler shift are restricted to $\tau_{\max} = 0.2T_0$ and $\nu_{\max} = 0.2F_0$, respectively. QAM/FBMC outperforms all other schemes. OFDM performs slightly worse, due to the broad characteristic of the rectangular waveform in the frequency domain. As mentioned above, OQAM/FBMC suffers from the phase difference of the channels and therefore has the worst performance in this scenario. In Fig. 7(b) also a second antenna is used at the relay. Here, OQAM/FBMC outperforms

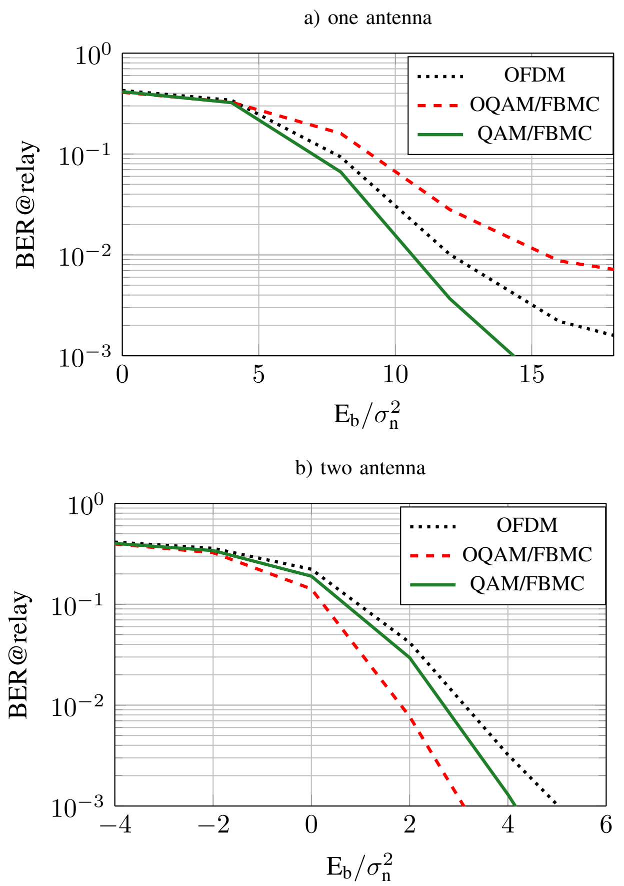

Fig. 7. BER performance at the relay of (a) one and (b) two antennas at the relay, with G-JCNC.

all other schemes offering the most robust design against huge distortions by doubly dispersive channels.

V. Summary and Outlook

In this paper we analyzed three different multi-carrier schemes and three different detection schemes within two phase TWRCs. The superposition of signals from both users leading to an under-determined system has a severe influence on the BER performance. Especially for OQAM, which is inherently sensitive against phase errors, the performance decreases dramatically, if the relay is equipped with only one antenna and the choice of the multi-carrier scheme should be QAM/FBMC, which outperforms all other schemes. In contrast, by introducing a second antenna OQAM modulation is the favorable choice in the TWRC in this setting.

VI. Acknowledgment

This work was supported in part by the German Research Foundation (DFG) under grant WU 499/10-1 within the priority program "Communication in Interference Limited Networks (COIN)", SPP 1397.

References

[1] B. Saltzberg, "Performance of an Efficient Parallel Data Transmission System," *Communication Technology, IEEE Transactions on*, vol. 15, no. 6, pp. 805–811, December 1967.

[2] J. Du, *Pulse Shape Adaptation and Channel Estimation in Generalised Frequency Division Multiplexing Systems*, Licentiate thesis in electronics and computer systems, KTH, Stockholm, Sweden, November 2008.

[3] S. Zhang, S.C. Liew, and P.P. Lam, "Hot Topic: Physical-layer Network Coding," in *MobiCom 06*, Los Angeles, CA, USA, 2006.

[4] I. W.-H. Ho, S.C. Liew, and L. Lu, "Feasibility Study of Physical-Layer Network Coding in 802.11p VANETs," in *The IEEE International Symposium on Information Theory 2014*, June 2014.

[5] M. Wu, F. Ludwig, M. Woltering, D. Wübben, A. Dekorsy, and S. Paul, "Analysis and Implementation for Physical-Layer Network Coding with Carrier Frequency Offset," in *International ITG Workshop on Smart Antennas (WSA2014)*, Erlangen, Germany, Mar 2014.

[6] S. Schedler, M. Woltering, D. Wübben, V. Kühn, and A. Dekorsy, "Investigation on Gaussian Waveforms to Improve Robustness in Physical Layer Network Coding," in *18th International OFDM Workshop 2014 (InOWo'14)*, 2014.

[7] M. Woltering, D. Wübben, A. Dekorsy, S. Schedler, and V. Kühn, "Physical Layer Network Coding Using Gaussian Waveforms: A Link Level Performance Analysis," in *10th International ITG Conference on Systems, Communications and Coding (SCC 2015)*, Hamburg, Germany, Feb 2015.

[8] M. Woltering, D. Wübben, and A. Dekorsy, "Physical Layer Network Coding with Gaussian Waveforms using Soft Interference Cancellation," in *IEEE 81th Vehicular Technology Conference (VTC2015-Spring)*, Glasgow, Great Britain, May 2015.

[9] G. Wunder, P. Jung, M. Kasparick, T. Wild, F. Schaich, Yejian Chen, S. Brink, I. Gaspar, N. Michailow, A. Festag, L. Mendes, N. Cassiau, D. Ktenas, M. Dryjanski, S. Pietrzyk, B. Eged, P. Vago, and F. Wiedmann, "5GNOW: Non-Orthogonal, Asynchronous Waveforms for Future Mobile Applications," *Communications Magazine, IEEE*, vol. 52, no. 2, pp. 97–105, February 2014.

[10] I. Daubechies, "The Wavelet Transform, Time-Frequency Localization and Signal Analysis," *Information Theory, IEEE Transactions on*, vol. 36, no. 5, pp. 961–1005, Sep 1990.

[11] M. Woltering, D. Wübben, and A. Dekorsy, "Factor Graph based Equalizer for Two Way Relaying Channels with General Waveforms," in *20th International ITG Workshop on Smart Antennas (WSA'2016)*, München, Germany, March 2016.

[12] D. Waldhauser, L. Baltar, and J. Nossek, "MMSE subcarrier Equalization for Filter Bank based Multicarrier Systems," *IEEE Workshop on Signal Processing Advances in Wireless Communications, SPAWC*, , no. Ici, pp. 525–529, 2008.

[13] U. Bhat and T.M. Duman, "Decoding Strategies for Physical-Layer Network Coding over Frequency Selective Channels," in *Wireless Communications and Networking Conference (WCNC), 2012 IEEE*, April 2012.

[14] M. Wu, D. Wübben, and A. Dekorsy, "Mutual Information Based Analysis for Physical-Layer Network Coding with Optimal Phase Control," in *Conference on Systems, Communication and Coding (SCC), Proceedings of 2013 9th International ITG*, Jan 2013.